

## Article

# Comparison of CO<sub>2</sub> Separation Efficiency from Flue Gases Based on Commonly Used Methods and Materials

Zenon Ziobrowski \* and Adam Rotkegel 

Institute of Chemical Engineering, Polish Academy of Sciences, 44-180 Gliwice, Poland; arot@iich.gliwice.pl

\* Correspondence: zenz@iich.gliwice.pl; Tel.: +48-322-310-811; Fax: +48-322-310-318

**Abstract:** The comparison study of CO<sub>2</sub> removal efficiency from flue gases at low pressures and temperatures is presented, based on commonly used methods and materials. Our own experimental results were compared and analyzed for different methods of CO<sub>2</sub> removal from flue gases: absorption in a packed column, adsorption in a packed column and membrane separation on polymeric and ceramic membranes, as well as on the developed supported ionic liquid membranes (SILMs). The efficiency and competitiveness comparison of the investigated methods showed that SILMs obtained by coating of the polydimethylsiloxane (PDMS) membrane with 1-ethyl-3-methylimidazolium acetate ([Emim][Ac]) exhibit a high ideal CO<sub>2</sub>/N<sub>2</sub> selectivity of 152, permeability of 2400 barrer and long term stability. Inexpensive and selective SILMs were prepared applying commercial membranes. Under similar experimental conditions, the absorption in aqueous Monoethanolamine (MEA) solutions is much faster than in ionic liquids (ILs), but gas and liquid flow rates in packed column sprayed with IL are limited due to the much higher viscosity and lower diffusion coefficient of IL. For CO<sub>2</sub> adsorption on activated carbons impregnated with amine or IL, only a small improvement in the adsorption properties was achieved. The experimental research was compared with the literature data to find a feasible solution based on commercially available methods and materials.

**Keywords:** carbon dioxide; absorption; adsorption; membrane separation



**Citation:** Ziobrowski, Z.; Rotkegel, A. Comparison of CO<sub>2</sub> Separation Efficiency from Flue Gases Based on Commonly Used Methods and Materials. *Materials* **2022**, *15*, 460. <https://doi.org/10.3390/ma15020460>

Academic Editors: Tański Tomasz and Przemysław Słopiński

Received: 16 November 2021

Accepted: 5 January 2022

Published: 8 January 2022

**Publisher's Note:** MDPI stays neutral with regard to jurisdictional claims in published maps and institutional affiliations.



**Copyright:** © 2022 by the authors. Licensee MDPI, Basel, Switzerland. This article is an open access article distributed under the terms and conditions of the Creative Commons Attribution (CC BY) license (<https://creativecommons.org/licenses/by/4.0/>).

## 1. Introduction

The observed growth of greenhouse gas emissions, mainly from fossil fuels combustion in industry, have stimulated the development of new technologies for CO<sub>2</sub> removal and storage [1,2].

European Union Emission Trading Scheme (EU ETS) is the biggest strategy to control greenhouse gas emissions with its carbon tax and carbon allowances [3,4]. In 2019, the carbon tax level was about 100 €/ton of CO<sub>2</sub> equivalent and the carbon allowance price level was above 30 €/ton of CO<sub>2</sub> equivalent [5]. Within the EU ETS control policy, greenhouse gas emissions should be 41% lower in 2030 than in 2005. The price of CO<sub>2</sub> emission allowances is rising and reached 60 €/ton CO<sub>2</sub> in 2021, even though it was predicted to reach 40 €/ton CO<sub>2</sub> by 2023 [6].

In order to regulate these emissions, carbon capture and storage (CCS) and carbon capture, utilization and storage (CCUS) techniques have been widely used [7,8]. The carbon dioxide capture and separation is the first step of these techniques and its cost is estimated to be as much as 80% of the total CCS cost [9,10]. An important part of CCUS is the carbon dioxide utilization step, which is regarded as the most challenging and has potential to reduce the world's current annual CO<sub>2</sub> emissions by 10% [11].

The main approaches for CO<sub>2</sub> capture are pre-combustion, post-combustion and oxy-combustion processes [12,13]. In post-combustion processes, CO<sub>2</sub> concentration in flue gas is about 10 to 15% vol., pressure is near atmospheric, and the temperature is usually in the range of 313–348 K [14]. The CO<sub>2</sub> concentrations and pressures are higher for CO<sub>2</sub> separation from natural gas [15].

Generally, the following methods have been used for carbon dioxide capture from gases: absorption, adsorption, membrane separation, cryogenic distillation, hydrate-based CO<sub>2</sub> capture, chemical-looping combustion and biological separation using bacteria or algae [11,16]. Among these methods, absorption, adsorption and membrane separation are regarded as the most established and mature.

### 1.1. Absorption

Currently, among the available separation methods, the amine scrubbing processes using MEA are widely used in coal-fired power plants for CO<sub>2</sub> capture [17,18]. It is the most advanced technology for CO<sub>2</sub> removal, and its advantage is high absorption efficiency (greater than 90%). Sorbents can be easily regenerated by heating or depressurization. The disadvantages being reported are degradation of amines with temperature and time, corrosion, amine losses by evaporation, toxicity of solvents used in absorption processes [19,20], high capital and operation costs [21], high energy requirement [22] and a high amount of heat for sorbent regeneration [23]. The sorbent regeneration for primary and tertiary amines may increase the total operating costs by up to 70% when the heat of the reaction is high [9,10].

It was reported by Ramdin et al. [24] that approximately 2.5–3.6 GJ is required to remove one ton of CO<sub>2</sub> using a 30 wt.% aqueous MEA solution. Lucquiaud et al. [25], Jackson and Brodal [26] have found that the energy required for a CCS plant is about 250–300 kWh/t CO<sub>2</sub>, whereas the estimated energy needed for CO<sub>2</sub> compression is 80–120 kWh/t CO<sub>2</sub>.

For a typical amine scrubbing process using MEA solution, the energy consumption is approximately 3.8 MJ/kg CO<sub>2</sub>, while the energy needed for regeneration is about 3.22 MJ/kg CO<sub>2</sub> [27]. Li et al. [28] reported that for amine scrubbing process the minimum reboiler duty is 3.1 MJ/kg CO<sub>2</sub>.

Optimizing important process parameters, the height of absorber, stripper, the reboiler duty could save about 20% of the heat consumption, thus improving the efficiency of the process [29–32].

In past decades, as an alternative to traditional amines, ionic liquids and deep eutectic solvents (DESs) have been considered as potential replacements for CO<sub>2</sub> capture [33–36].

Their properties—tunability, chemical and thermal stability, high CO<sub>2</sub> solubility, negligible vapor pressure, and a more environmentally friendly character—allow them to be used as alternative CO<sub>2</sub> absorbents. The literature reviews show a variety of synthesized ILs [37,38] and DESs [39–41] for CO<sub>2</sub> capture and the need to look for a reliable screening procedure linking molecular characteristics of ILs and DESs to their overall performance in carbon capture processes.

The proper selection of individual IL components and molar ratios in the case of DESs may allow us to prepare a specific and unique solvent that is suited for a particular application. A major issue in the case of IL applications, especially in comparison with low-cost DESs, are their high viscosity and price. Most of the investigated ILs absorb CO<sub>2</sub> physically. This mechanism is responsible for a low CO<sub>2</sub> loading and an easier CO<sub>2</sub> desorption than in the case of MEA solutions [42].

Compared to amine-based solvents, conventional ILs exhibit a low CO<sub>2</sub> absorption capacity. The CO<sub>2</sub> solubility in post-combustion processes is less than 5% mol., as a result of low partial pressure of CO<sub>2</sub> at post-combustion conditions [43]. In order to increase the CO<sub>2</sub> absorption capacity in ILs, new task-specific ionic liquids (TSILs) were developed, as functionalized ILs, by introducing an amino group (NH<sub>2</sub>) into the IL. In functionalized ILs, as opposed to conventional ILs, CO<sub>2</sub> absorption occurs by chemical reaction and the CO<sub>2</sub> loading capacity is comparable to MEA solution.

In 2009, Bara et al. [44] obtained a CO<sub>2</sub> loading capacity comparable to that of an MEA solution, which represents an interesting alternative to amine scrubbing processes [36,45–47]. Shifflet et al. [48,49] investigated the CO<sub>2</sub> phase behavior in imidazolium-based ILs [Bmim][Ac]

and [Emim][Ac]. They found that these ionic liquids containing acetate anion showed a strong CO<sub>2</sub> absorption at pressure 2 MPa and in the temperature range of 10–75 °C.

The presence of an amine moiety in the anion [50,51] or in anion and cation [52] of imidazolium-based ILs increased CO<sub>2</sub> absorption capacities of the corresponding conventional ILs. The positioning of the amine moiety at the cation of IL or at the anion of IL enables carbamate formation with 1:2 or 1:1 reaction stoichiometry, respectively.

Shiflett et al. used [Bmim][Ac] as a CO<sub>2</sub> absorbent, and performed the simulation of the CO<sub>2</sub> separation process and compared it with the MEA-based scrubbing process. They reported that [Bmim][Ac] can replace an MEA solution in a coal-fired power plant (180 MW). Compared to the MEA-based scrubbing process, the energy losses were lowered by 16% and the investment costs by 11% [53].

It was found that using [Emim][Ac] in the process of carbon dioxide removal from flue gas, the energy requirements were lower but the investment costs were higher in comparison with the MEA-based process [54]. There are several pilot projects based on ionic liquids, yet capture data are unavailable.

### 1.2. Adsorption

Adsorption is another recommended method for CO<sub>2</sub> capture from post-combustion gases because of its high adsorption capacity and efficiency, which is greater than 85%, its low capital investments, its lower regeneration energy requirements and its ease of handling. The achieved purity of CO<sub>2</sub> can be higher than 95% [55–57]. Moreover, the process is reversible. The regeneration step may be realized by vacuum, pressure, or temperature swing adsorption (VSA, PSA, TSA) [58].

Many different adsorbents were investigated: zeolites, mesoporous silica, clays, metal-organic frameworks (MOFs) and activated carbons [59]. These adsorbents are not widely used for economical and technical reasons; high desorption energy and high temperature adsorbents are required.

Porous-activated carbons exhibit better adsorption than other adsorbents, their energy consumption at the regeneration step is low, and for this reason activated carbons are often used in industry [60].

A great research effort was directed to develop proper surface and pore structures as well as new functionalized activated carbons to obtain enhanced CO<sub>2</sub> adsorption capacity and optimize the breakthrough time [61].

He et al. [62] investigated the dynamic of adsorption of gas containing 15% CO<sub>2</sub> vol. on coconut-shell-activated carbons before and after grafting and impregnation with novel phosphonium-based IL for different gas flow rates and adsorption pressures. They found that the CO<sub>2</sub> adsorption capacity of the investigated activated carbons at 0.1 MPa and 25 °C had changed from 10 to 7 wt.% after functionalization with IL, while and ideal CO<sub>2</sub>/N<sub>2</sub> selectivity had distinctly increased from 7 to 30.

Mesoporous silica are materials that are frequently used for adsorbent preparation because of their easily modifiable structural properties [63]: high surface area, large, tunable pore diameter volume. Silica showed a rather low CO<sub>2</sub> adsorption, but the addition of amino groups to silica support allow for silica modification and development of functionalized adsorbents for CO<sub>2</sub> [64]. The functionalization method is of great importance in CO<sub>2</sub> adsorption. The objective of the functionalization method makes for an improvement of the adsorption capacity by introducing specific groups to the surface of the adsorbent. This can be done by a grafting technique or by a chemical impregnation technique under dry or wet conditions.

In the grafting method, the specific groups are bonded chemically through covalent bonding to the solid support. Thus, modified silica acquire more stable properties and faster kinetics because of their stronger interactions. Hiremath et al. [65] used 1-methyl-3-ethylimidazolium-based IL grafted on mesoporous silica functionalized with Lysine-IL and found a CO<sub>2</sub> adsorption capacity of 0.61 mmol/g-adsorbent at 298 K.

Zhang et al. [66] found a CO<sub>2</sub> adsorption capacity of 2.15 mmol/g-adsorbent at 333 K and 0.15 bar using a wet impregnation method. They impregnated functionalized mesoporous silica SBA-15 with tetraethylenepentaammonium nitrate ([TEPA][NO<sub>3</sub>]).

The impregnated silica have a greater adsorption capacity than grafted silica [67].

Solid adsorbents developed through amine-functionalization adsorbed CO<sub>2</sub> by chemisorption and follow the carbamate formation scheme. The reported CO<sub>2</sub> adsorption capacities are in the wide range from 0.1 to 5.91 mmol/g-adsorbent depending on experimental conditions and investigated materials. The typical enthalpy values for chemisorption and for physical adsorption are between 40 and 90 kJ/mol and between 15 and 40 kJ/mol, respectively [67]. This means that CO<sub>2</sub> molecules are more strongly bound to the surface of amine-functionalized solid adsorbents by both chemical reactions and physical interactions with silica support [68]. For raw silica materials, physical adsorption takes place mainly via van der Waals interactions.

### 1.3. Membrane Separation

Membrane gas separation is one of the most mature and advanced methods for gas separation. It is considered as an alternative method for carbon dioxide removal in relation to the amine-based scrubbing processes. Its advantages are low energy demands, simple maintenance [69,70], an environmentally friendly character, low cost of the polymeric membranes and its variety of manufacturers [71,72]. The obstacles are low permeability and selectivity, poor stability, aging, swelling and sensitivity to the content of impurities and water [73,74].

Different materials (organic and inorganic) were tested for CO<sub>2</sub> separation [75,76]. A commonly used cellulose acetate, polyimides, fluorinated polyimides, polyether-urethane-urea, polyether-block-amide show low permeability in the range from 2.4 to 212 and low ideal CO<sub>2</sub>/N<sub>2</sub> selectivity ( $\alpha_{\text{CO}_2/\text{N}_2}$ ) in the range from 12.5 to 36.7 [77–82]. New advanced polymeric materials with CO<sub>2</sub> separation potential are presented and studied such as polymers with intrinsic microporosity (PIM) or thermally rearranged polymers (TR); however, their application needs more research [83].

It was found that common PDMS membranes provide a high permeability and can be used for carbon dioxide capture from post-combustion gases [84,85]. These membranes keep their properties and do not undergo swelling or degradation [86]. The PDMS membranes possess a very high CO<sub>2</sub> permeability of 4000 barrer but a low ideal CO<sub>2</sub>/N<sub>2</sub> selectivity of 2.6 [87].

In previous years, SILMs have been used for selective gas separation. SILMs may be developed by impregnation of the porous support with an ionic liquid. The application of ILs for CO<sub>2</sub> removal averts the shortcomings of amine-based processes [88,89]. Ionic liquids have properties such a high carbon dioxide solubility, a negligible vapor pressure, and thermal stability, which allow them to be used as effective carbon dioxide absorbents. The application of ILs in carbon dioxide absorption may result in significant investment and operation cost reduction [90,91]. Unfortunately, their high viscosities and prices are their important disadvantages.

Different membrane supports made of polymeric or inorganic materials and different ILs have been tested. Cserjési et al. [92] investigated hydrophilic polyvinylidene fluoride (PVDF) support and 12 different room temperature ionic liquid RTILs. For prepared SILMs, the measured CO<sub>2</sub> permeabilities were from 94 to 750 barrer and  $\alpha_{\text{CO}_2/\text{N}_2}$  from 10.9 to 52.6. Santos et al. [93] also used PVDF support and prepared SILMs by impregnating PVDF with the following ionic liquids: 1-ethyl-3-methylimidazolium acetate ([Emim][Ac]), 1-butyl-3-methylimidazolium acetate ([Bmim][Ac]) and vinylbenzyltrimethylammonium acetate ([Vbtma][Ac]). For investigated ILs in the temperature range from 25 to 60 °C, they found carbon dioxide permeability from 852 to 2114 barrer and ideal CO<sub>2</sub>/N<sub>2</sub> selectivity from 26.4 to 39.

Bara et al. [94] studied imidazolium-based room temperature ionic liquids (RTILs) and found carbon dioxide permeability in the range from 210 to 320 barrer and ideal CO<sub>2</sub>/N<sub>2</sub> selectivity from 16 to 26.

Albo et al. [95] used [Emim][Ac] to impregnate porous Al<sub>2</sub>O<sub>3</sub>/TiO<sub>2</sub> tubes. The measured CO<sub>2</sub> permeability and ideal selectivity were 780 barrer and 35.4, respectively. Sánchez Fuentes et al. [96] investigated functionalized ceramic SILMs with amino group at the anionic part of IL. They obtained a high CO<sub>2</sub> permeability of 3000 barrer and high  $\alpha_{\text{CO}_2/\text{N}_2}$  of 70.

Khraisheh et al. [97] used microporous polysulfone matrix (PSF) impregnated with different concentrations of ionic liquids: 1-Ethyl-3-methylimidazolium hexa fluorophosphate ([Bmim][PF<sub>6</sub>]) and bis(trifluoromethylsulfonyl) imide ([Emim][Tf<sub>2</sub>N]). The small addition of IL to the PSF matrix enhanced both CO<sub>2</sub> permeability and selectivity. The measured CO<sub>2</sub> permeabilities were from 10.8 to 13.8 barrers and  $\alpha_{\text{CO}_2/\text{N}_2}$  from 33 to 37.2. The correct impregnation is very important for the stability of the liquid phase in an SILM [98].

The goal of this work is to present and compare the competitiveness and efficiency of CO<sub>2</sub> separation from flue gases based on commonly used methods and materials. Our own experimental study of CO<sub>2</sub> removal from post-combustion gases is presented for different methods at low pressures (1–5 bar) and temperatures (20–60 °C). The following advanced CO<sub>2</sub> capture methods were compared: absorption and adsorption in a packed column and membrane separation on ceramic and polymeric membranes, as well as on developed SILMs.

Packed columns are the standard technical solution used in many industrial processes. However, large capital costs and the size of apparatus are limiting factors for an efficient application of this technology. The membrane processes permit the removal of these limitations. This technology is often used in industry and is considered environmentally friendly; it does not emit any gases or liquids.

This work also presents the comparison of the separation efficiency for SILMs prepared by impregnation of the ceramic support of commercial membranes made by INOPOR and Pervatech BV with ionic ILs: [Emim][Ac], [Bmim][Ac], [Emim][Tf<sub>2</sub>N] and [Emim][BF<sub>4</sub>]. The aim of this part of the research was to determine the stability and separation enhancement for SILM developed by the addition of an IL-separating layer to commercial membranes.

Additionally, the experimental research is compared with the literature data to find a feasible, economically reasonable and environmentally friendly solution based on commercially available methods and materials.

## 2. Experimental Results and Discussion

Experimental research is presented for the following CO<sub>2</sub> capture methods: absorption, adsorption and membrane separation. The experiments were carried out on experimental setups described in detail in previous works [99–101]. The main parts of the experimental setups were packed columns with CO<sub>2</sub> liquid solvents or solid adsorbents and a membrane separation module with ceramic and polymeric membranes, as well as the developed SILMs.

### 2.1. Absorption in a Packed Column

A 15 wt.% MEA solution [Emim][Ac] and [Bmim][Ac] were used as the solvents for CO<sub>2</sub> absorption in a packed column sprayed with IL. [Emim][Ac] and [Bmim][Ac] were taken into account due to literature reports about their high absorption capacity and chemical type of absorption (chemisorption).

For these solvents, the sorption capacity and the time of complete saturation with CO<sub>2</sub> was determined using a bubble-type apparatus [99]. This apparatus consisted of a thermostatic 2 dm<sup>3</sup> glass reactor, a mixer and a gas bubbler. Carbon dioxide was introduced at the bottom of the glass reactor and was absorbed in the MEA solution or ionic liquid at temperatures 20, 40, 60 °C and atmospheric pressure.

The CO<sub>2</sub> absorption capacity,  $S$ , in the investigated solvents was calculated as a ratio of the absorbed mass of CO<sub>2</sub> [kg] and the mass of the solvent absorbing CO<sub>2</sub> [kg]. The results are shown in Figure 1 [99].

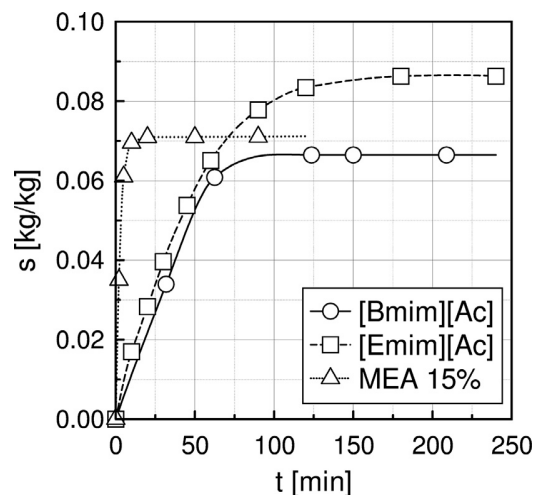


**Figure 1.** The CO<sub>2</sub> sorption capacity at 1 bar, temperature 40 °C, gas flow rate  $V_g = 36$  L/h.

At the temperature of 40 °C, atmospheric pressure and gas flow rate  $V_g = 36$  L/h, the CO<sub>2</sub> absorption capacities for [Bmim][Ac] and [Emim][Ac] were 0.067 and 0.086 [kg<sub>CO2</sub>/kg<sub>IL</sub>] respectively. In the same conditions, the absorption capacity for 15 wt.% MEA was close to these values, 0.071 [kg<sub>CO2</sub>/kg<sub>MEA</sub>]. Similar results were reported in the literature (0.077 and 0.079 for [Bmim][Ac] and [Emim][Ac], respectively) [45]. Additionally, it can be seen in Figure 1 that the absorption profile for MEA is steeper than for IL, which indicates that the CO<sub>2</sub> absorption rate in MEA is higher than in both ILs.

The obtained comparable results of CO<sub>2</sub> absorption capacity in selected ionic liquids and MEA solutions led to an attempt to use these ionic liquids as CO<sub>2</sub> absorbents in a packed column. The experimental setup described in [100] consisted of a packed glass column with an inner diameter of 0.05 m, a length of 0.35 m filled with glass Rashig rings of a diameter  $5 \times 1$  mm and a length of 5 mm. The column was heated with a water jacket. The ionic liquid or MEA solution flowed through the bed and absorbed CO<sub>2</sub> from the gas mixture in co-current or countercurrent flow. The experiments were carried out at atmospheric pressure and in temperatures of 20, 40 and 60 °C.

The CO<sub>2</sub> absorption in ILs was performed in a limited range of flow rates to avoid flooding of the column. In the co-current flow (gas 1–2.3 L/min and liquid 0.05–0.2 L/min) and in the countercurrent flow (gas 1–2.1 L/min and liquid 0.05–0.1 L/min). The absorption temperature determines the efficiency of CO<sub>2</sub> capture. The minimum absorption temperature was set at 40 °C because [Bmim][Ac] solidifies at 30 °C.

The regeneration step (desorption process) was carried out at the temperature 90 °C, using pure nitrogen to help stripping CO<sub>2</sub>. The regenerated IL was used again. In the case of MEA, for each experiment, new 15 wt.% MEA-water solution was used. The amount of absorbed CO<sub>2</sub> in the absorption process (3–4 h) and amount of desorbed CO<sub>2</sub> in desorption process (6–8 h) was controlled gravimetrically until measured changes were negligible (0.1 g).

The experimental results are presented in Figures 2 and 3. The comparison of carbon dioxide absorption in the investigated solvents is presented in Figure 2 for co-current flow, inlet CO<sub>2</sub> concentration 15% vol. and absorption temperature of 40 °C and gas flow rate  $V_g = 36$  L/h. The outlet CO<sub>2</sub> concentration,  $C_{out}$ , after passing through the column, is low at the beginning because in the liquid phase there is no CO<sub>2</sub> and almost all CO<sub>2</sub> in the gas phase is absorbed. With time, the amount of CO<sub>2</sub> absorbed in liquid decreases and thus the outlet CO<sub>2</sub> concentration rises until complete saturation, when  $C_{out} = C_{in}$ . The experiments were carried out until  $C_{out} = (0.90–0.98) C_{in}$ . For ILs, the initial outlet

CO<sub>2</sub> concentration is higher and the time when concentration  $C_{out}/C_{in} \geq 0.95$  is longer in comparison with the 15 wt.% MEA solution.

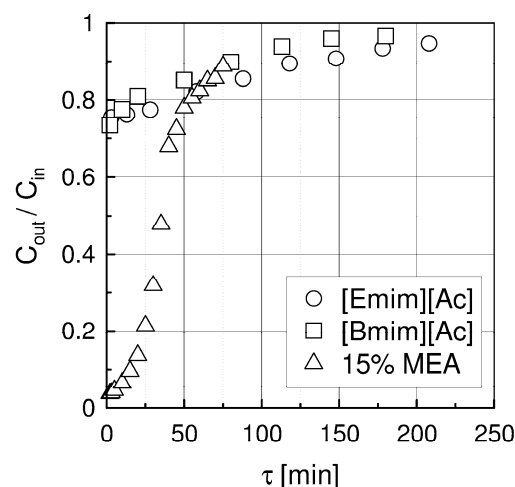


**Figure 2.** Comparison of outlet CO<sub>2</sub> concentrations for [Emim][Ac], [Bmim][Ac] and 15 wt.% MEA at 1 bar, temperature 40 °C,  $C_{in} = 15\%$  vol. and gas flow rate  $V_g = 138$  L/h.

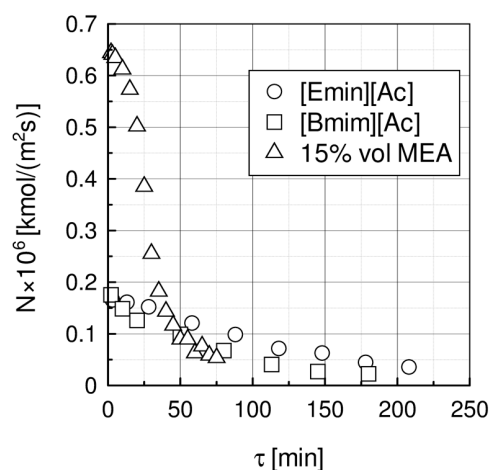


**Figure 3.** Comparison of molar fluxes of absorbed CO<sub>2</sub> for investigated liquids at 1 bar, temperature 40 °C,  $C_{in} = 15\%$  vol. and gas flow rate  $V_g = 138$  L/h.

The measured initial outlet CO<sub>2</sub> concentration  $C_{out}/C_{in}$  are: 0.035, 0.721 and 0.754 for MEA solution, [Bmim][Ac] and [Emim][Ac], respectively. The time needed to reach outlet CO<sub>2</sub> concentration  $C_{out} = 15\%$  vol. is about 80 min for MEA solution and 210 min for [Emim][Ac] and [Bmim][Ac].

The influence of absorption temperature and flows direction on outlet CO<sub>2</sub> concentration is of minor effect.

In Figure 3, the measured CO<sub>2</sub> molar fluxes are compared. The initial CO<sub>2</sub> molar flux for 15 wt.% MEA solution is significantly higher and decreases faster with time than for ILs.

Experimental results show that imidazolium-based ionic liquids can be applied in a packed column for CO<sub>2</sub> removal from post-combustion gases.

In Table 1, physical parameters of the CO<sub>2</sub> absorption in a packed column are presented for: temperature 40 °C, co-current flow, inlet CO<sub>2</sub> concentration 15% vol.

The viscosities of both ILs are very high and as a consequence, mass transfer coefficients in the liquid phase are much lower than for 15 wt.% MEA.

**Table 1.** The physical parameters of the CO<sub>2</sub> absorption process in a packed column.

Liquid	$\rho$ kg/m <sup>3</sup>	$\eta \times 10^3$ Pa s	$D_{\text{CO}_2} \times 10^{10}$ m <sup>2</sup> s <sup>-1</sup>	$k_L \times 10^8$ kmol/(m <sup>2</sup> s)	$k_G \times 10^8$ kmol/(m <sup>2</sup> s)	$N_{\text{exp}, \tau=0} \times 10^6$ kmol/(km <sup>2</sup> s)	S kg/kg	Price <sup>*)</sup> €/kg
[Emim][Ac]	1.025	66.98	4.21	9.90	3.08	0.166	0.053	350
[Bmim][Ac]	1.050	145.3	2.51	6.04	3.08	0.177	0.043	460
15% MEA	0.999	0.938	22.4	204	3.08	0.668	0.049	20

<sup>\*)</sup> prices by Proionic <https://proionic.com> (accessed on 5 November 2021).

Comparison of mass transfer coefficients in liquid and gas phase shows that the CO<sub>2</sub> absorption process in a packed column is controlled by a liquid side mass transfer resistance. The liquid side mass transfer coefficient, as well as the initial CO<sub>2</sub> molar flux for [Bmim][Ac] and [Emim][Ac] are several times lower than for 15 wt.% MEA solution. Absorption capacities, S, are comparable for all of the investigated liquids.

## 2.2. Adsorption in a Packed Column

The adsorptive CO<sub>2</sub> removal research was carried out on an experimental setup equipped with a stainless steel column of diameter 50 mm and length 800 mm. The column was thermostated by Thermostat Lauda Eco Gold with accuracy  $\pm 0.2$  °C. The following beds were investigated: molecular sieves type 4A (4 mm) made by Chempur, pelletized activated carbon (4 mm) made by Elbar-Katowice Sp z o.o. and pelletized activated coconut carbon (4 mm) impregnated with triethylenediamine (TEDA)—PHS 4S TEDA made by Eurocarb Products Limited and granulated activated coconut carbon (2 mm). The height of the investigated beds was about 700 mm.

To measure CO<sub>2</sub> concentrations, a gas chromatograph Varian Star 3800 and PORAPLOT Q 25 m long megabore column and TCD detector was used for GC component analysis with accuracy  $\pm 0.01\%$ .

Before measurements, the bed was heated in an electric oven at the temperature of 120 °C for 24 h. The prepared CO<sub>2</sub>/N<sub>2</sub> gas mixture with CO<sub>2</sub> concentration in the range of 3–12% vol. was preheated to the column temperature and introduced at the bottom of the column. Flow meter and rotameters with accuracy  $\pm 20$  mL/min were used to measure gas flow rates. Pure gases CO<sub>2</sub> and N<sub>2</sub> (purity 99.99%) were used to prepare an inlet gas mixture. At the top and bottom of the column and gas inlet/outlet, NiCr-Ni thermocouples with accuracy  $\pm 0.2$  °C were used to measure and control the temperatures of the bed.

The inlet/outlet CO<sub>2</sub> concentrations were measured with time to determine the amount of CO<sub>2</sub> adsorbed in the bed. Additionally, the bed was weighed before and after the experiments to control concentration measurements.

To improve the CO<sub>2</sub> removal, the beds were later impregnated with ionic liquid [Emim][Ac]. The impregnation was made by soaking the previously heated bed in 50 wt.% IL-isopropanol solution for 24 h. Thus, the prepared bed was dried and heated for the next 48 h and then used in experiments at an atmospheric pressure.

The experimental results are presented in Figures 4 and 5 for pelletized activated carbon (4 mm) made by Elbar-Katowice Sp z o.o. and pelletized activated coconut carbon (4 mm) impregnated with TEDA made by Eurocarb Products Limited for the temperature of 20 °C and  $C_{\text{in}} = 10\%$  vol.

In Figure 4, pelletized activated carbon (4 mm) impregnated with ionic liquid [Emim][Ac] has a slightly higher sorption capacity than pelletized activated carbon (4 mm) without impregnation. Furthermore, breakthrough of the column bed occurs later in the case of pelletized activated carbon (4 mm) impregnated with IL. If it is assumed that the column breakthrough occurs when the outlet concentration reaches 10% of the inlet concentration value, then for the column packed with activated carbon without IL, the breakthrough time is 4.6 min, and for the same column impregnated with IL, the breakthrough time was increased to 7.6 min. Unfortunately, the improvement of CO<sub>2</sub> absorption capacity and capability of CO<sub>2</sub> removal is not satisfactory.

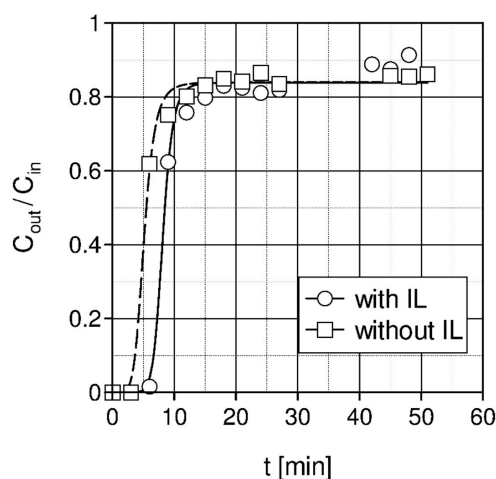


**Figure 4.** Comparison of measured CO<sub>2</sub> concentration for adsorption on pelletized activated carbon (4 mm) bed before and after its impregnation with ionic liquid [Emin][Ac] (1 bar, temperature 20 °C, C<sub>in</sub> = 10% vol. and gas flow rate V<sub>g</sub> = 750 L/h).

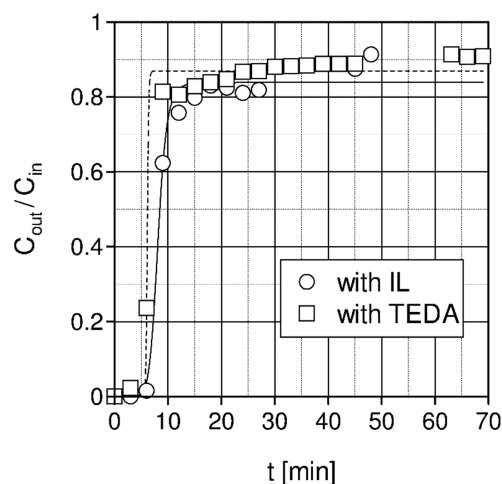


**Figure 5.** Comparison of measured CO<sub>2</sub> concentration for adsorption on pelletized activated carbon (4 mm) bed impregnated with ionic liquid [Emin][Ac] and on pelletized activated carbon coconut (4 mm) bed impregnated with TEDA amine (1 bar, temperature 20 °C, C<sub>in</sub> = 10% vol. and gas flow rate V<sub>g</sub> = 750 L/h).

Figure 5 presents a comparison of the measured outlet CO<sub>2</sub> concentration for adsorption of the inlet gas containing 10% vol. of carbon dioxide (C<sub>in</sub> = 10% vol.) on pelletized activated carbon (4 mm) impregnated with IL [Emin][Ac] and on pelletized-activated coconut carbon (4 mm) impregnated with amine TEDA. The CO<sub>2</sub> sorption capacity results obtained in both beds are similar and are equal to  $S = 0.013$  [kg<sub>CO2</sub>/kg<sub>adsorbent</sub>] for pelletized activated carbon (4 mm) impregnated with [Emin][Ac] and  $S = 0.012$  [kg<sub>CO2</sub>/kg<sub>adsorbent</sub>] for pelletized activated carbon (4 mm) impregnated with TEDA. He et. al. [62] reported adsorption capacity obtained in a fixed bed column (7 mm inner diameter and 150 mm in height) for activated carbon impregnated with phosphonium ionic liquid at 2 atm and 25 °C equal 0.029 [kg<sub>CO2</sub>/kg<sub>adsorbent</sub>]. The column breakthrough time defined above is similar and was 5.3 and 7.6 min for TEDA and [Emin][Ac], respectively.

The shape of the column breakthrough curve indicates that in the case of TEDA, the adsorption capacity of the bed is slightly lower, while the diffusion rate is much higher than in the case of an ionic liquid.

Research carried out on activated carbon impregnated with ionic liquids showed a slight increase in the sorption capacity of the modified adsorbents, as well as a slight

increase in their CO<sub>2</sub> adsorption properties. This may be due to the blockage of adsorbent pores by a viscous ionic liquid.

The regeneration of the bed was carried out in an electric oven at the temperature of 120 °C for 24 h.

### 2.3. Membrane Separation

The membrane separation research was carried out on the experimental setup, described in detail in our previous work [101]. The main part of the setup is a stainless steel module with a tubular ceramic membrane. The following commercial tubular ceramic membranes with outer diameter of 0.1 m, an inner diameter of 0.007 m, and a length 0.25 m were used in this research:

A—membranes made by Inopor with active TiO<sub>2</sub> layer and pore diameters 10, 30, 100 nm;

B—membranes made by Inopor with active Al<sub>2</sub>O<sub>3</sub> layer and pore diameters 5, 10 nm (γ-Al<sub>2</sub>O<sub>3</sub>) and 70 nm (α-Al<sub>2</sub>O<sub>3</sub>);

C—membranes made by Pervatech with active PDMS layer and pore diameter of ceramic support 100 nm.

Ionic liquids were purchased from Sigma-Aldrich: [Emim][Ac] (97.8%), [Bmim][Ac] (95%), [Emim][Tf<sub>2</sub>N] (95%), [Emim][BF<sub>4</sub>] (97%). Before the experiments, ILs were purified by vacuum for about 24 h.

In Table 2, some physical and thermal ILs properties are presented in standard conditions.

**Table 2.** Physical and thermal properties of ILs (0.1 MPa, 298.15 K).

Liquid	M kg/kmol	ρ kg/m <sup>3</sup>	η × 10 <sup>3</sup> Pa s	CO <sub>2</sub> Solubility % mol.	D <sub>CO<sub>2</sub></sub> × 10 <sup>10</sup> m <sup>2</sup> s <sup>-1</sup>	Price *) €/kg
[Emim][Ac]	170.21	1.025	66.98	26.7	4.21	350
[Bmim][Ac]	198.26	1.050	145.3	19.4	2.51	460
[Emim][BF <sub>4</sub> ]	197.97	1.27	34.0	2.0	5.95	620
[Emim][Tf <sub>2</sub> N]	391.31	1.52	32.6	3.0	5.6	690

\*) prices by Proionic <https://proionic.com> (accessed on 5 November 2021).

Significant differences in solubility values between presented ILs can be attributed to a different absorption mechanism: chemisorption in case of [Emim][Ac] and [Bmim][Ac] or physisorption in case of [Emim][BF<sub>4</sub>] and [Emim][Tf<sub>2</sub>N]. To immobilize IL in the pores of the ceramic membrane support, two impregnation methods were applied: coating and soaking.

The mass of IL added to the membrane was controlled by weighing of the membrane before and after impregnation. Similarly, before and after each series of experiments, the membrane was weighted to control its mass or weight loss.

Ideal CO<sub>2</sub>/N<sub>2</sub> selectivity was calculated according to Equation (1).

$$\alpha_{\text{CO}_2/\text{N}_2} = \frac{P_{\text{CO}_2}}{P_{\text{N}_2}} \quad (1)$$

where  $P_i$  is the permeability of component  $i$  [kmol m<sup>-1</sup> s<sup>-1</sup> Pa<sup>-1</sup>],  $P_i$  is a product of diffusivity ( $D_i$ ) and solubility ( $s_i$ ) of the component  $i$ .

Molar flux ( $N_i$ ) [kmol m<sup>-2</sup> s<sup>-1</sup>] for gas  $i$  was calculated according to Equation (2):

$$N_i = \frac{D_i s_i}{l} \Delta p = \frac{P_i}{l} \Delta p \quad (2)$$

where  $l$  is the membrane thickness [m],  $\Delta p_i$  is the pressure difference [Pa].

CO<sub>2</sub> and N<sub>2</sub> gases of purity 99.99% were used. When the membrane module was prepared and ready for experiments (residual gases were removed under vacuum, the required temperature was achieved), the pressure of feed gas was increased up to 500 kPa with 50 kPa steps. A Varian Digital flow meter was used to measure gas flow through the membrane. The measurements were repeated for both feed gases: N<sub>2</sub> and CO<sub>2</sub>.

Based on the chosen membranes A, B, and C, the SILMs were developed by impregnation with different ILs: [Emim][Ac], [Emim][Tf<sub>2</sub>N], [Emim][BF<sub>4</sub>] by coating and soaking methods. The effects of pressure, temperature, pore diameter and impregnation method on CO<sub>2</sub>/N<sub>2</sub> separation were investigated [101]. Some experimental separation results are presented in Figures 6–9.

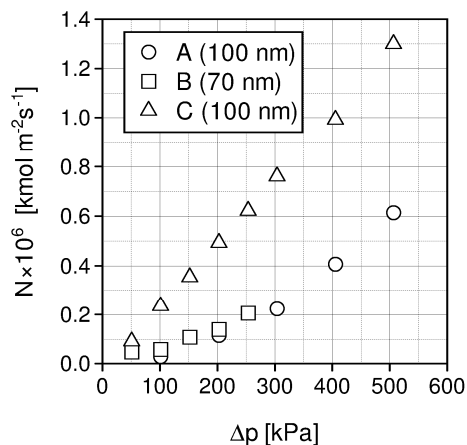


**Figure 6.** Comparison of CO<sub>2</sub> molar fluxes for SILMs based on membranes A, B and C impregnated with [Emim][Ac], temperature 20 °C.

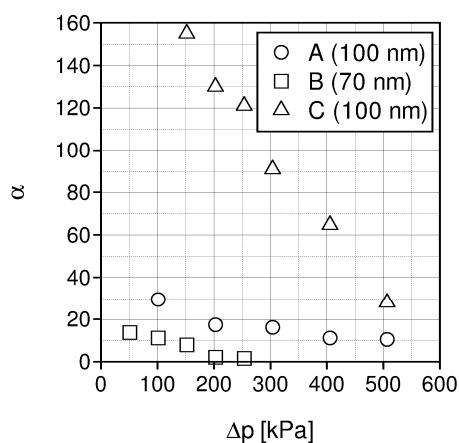


**Figure 7.** Ideal CO<sub>2</sub>/N<sub>2</sub> selectivity for SILMs based on membranes A, B and C impregnated with [Emim][Ac], temperature 20 °C.

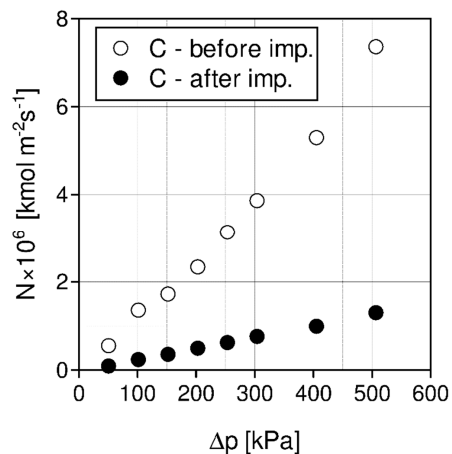


**Figure 8.** Carbon dioxide molar fluxes for membrane C (PDMS) before and after impregnation with [Emim][Ac], temperature 20 °C.

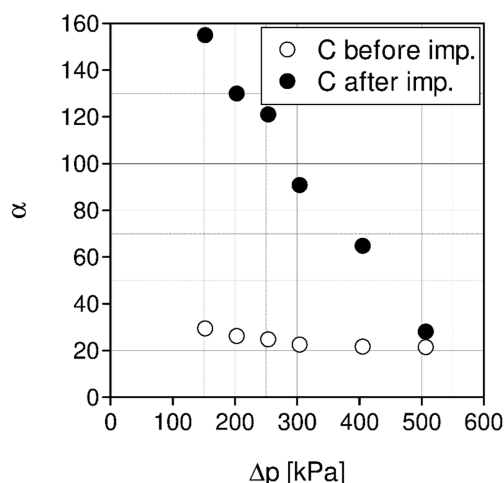


**Figure 9.** Ideal  $\text{CO}_2/\text{N}_2$  selectivities for membrane C (PDMS) before and after impregnation with [Emim][Ac], temperature 20 °C.

In Figure 6, carbon dioxide molar fluxes are presented for the developed SILMs, prepared by coating of the membranes A, B, C with [Emim][Ac].

The measured  $\text{CO}_2$  molar fluxes, for membrane C (PDMS) after impregnation, are distinctly greater than molar fluxes for membranes A and B in the same experimental conditions. Nitrogen molar fluxes were very small and were not presented in Figure 6. The differences between  $\text{CO}_2/\text{N}_2$  molar fluxes may be explained by a permeation mechanism, which for  $\text{N}_2$  is controlled by diffusivity, but for  $\text{CO}_2$  is controlled by  $\text{CO}_2$  solubility in IL. With the rising pressure difference, the driving force is rising and thus the measured  $\text{CO}_2$  molar fluxes also increase.

As can be seen in Figure 7, with the rising pressure, the ideal  $\text{CO}_2/\text{N}_2$  selectivities decrease. In the case of the SILMs prepared by impregnating the membrane C (PDMS), high selectivities were obtained.

The greatest measured ideal  $\text{CO}_2/\text{N}_2$  selectivities for SILMs based on membrane A and B are equal 30 and 15, respectively, and are significantly lower than for membrane C (PDMS), at about 152.

In Figure 8, carbon dioxide molar fluxes are presented for the same membrane C (PDMS) before and after impregnation with [Emim][Ac] for the temperature of 20 °C. As can be noticed, after impregnation, the  $\text{CO}_2$  molar fluxes are considerably lower because of additional mass transfer resistances of the IL layer.

High ideal  $\text{CO}_2/\text{N}_2$  selectivities measured for a SILM developed by coating with [Emim][Ac] of the membrane C (PDMS) can be explained by the effect of an additional layer formed by impregnating the ceramic tube with [Emim][Ac]. High selectivity is also proof that the coating method in this case is an efficient and economically reasonable way of preparing a highly selective SILM. [Emim][Ac] does not dissolve in PDMS. The impenetrable PDMS layer keeps the ionic liquid in the pores of the support, thus helping to maintain long-term stability and improving the performance of the prepared SILM. The separation mechanism may be described as resistance in a series model [93] with a  $\text{CO}_2$  chemical absorption in the IL layer and  $\text{CO}_2$  solution-diffusion in the PDMS layer.

The measured ideal selectivities are much higher after impregnation of the membrane C (PDMS) with ionic liquid [Emim][Ac], Figure 9.

The low cost and stability of the thus prepared SILM is an interesting alternative compared to SILMs based on expensive materials and advanced functionalized ILs [83,96].

The thickness of the PDMS layer—30  $\mu\text{m}$ —was given by the manufacturer. The IL layer thickness was estimated to be 210  $\mu\text{m}$  for coating and 450  $\mu\text{m}$  for soaking, taking into account the membrane weight after impregnation.

A proper realization of the coating process may help to achieve a better separation performance of the prepared SILMs [95].

In Figure 10, the developed SILMs were compared with the literature data for polymeric [92,93,102,103] and ceramic [95,96,104–106] SILMs, as well as the revised upper bound Robeson correlation (2008) [107]. The experimental results lying above this correlation are considered an improvement in separation efficiency of the investigated SILMs.

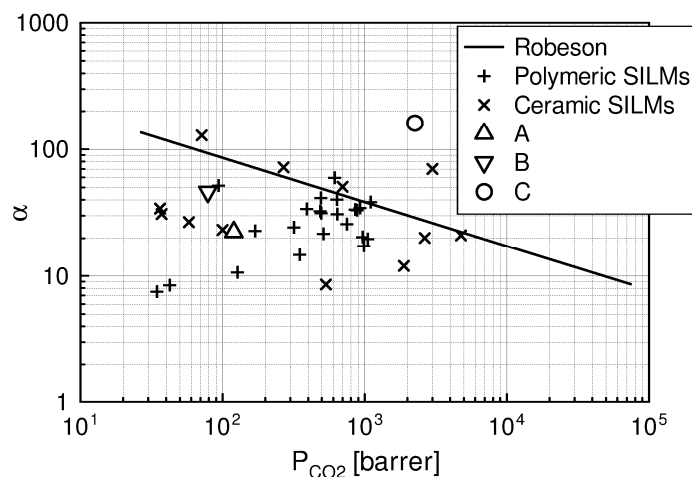


**Figure 10.** Separation performance comparison for investigated SILMs and literature data: A—Membrane A impregnated with [Emim][Ac], B—Membrane B impregnated with [Emim][BF<sub>4</sub>], C—Membrane C (PDMS) impregnated with [Emim][Ac].

The best results were obtained for SILMs based on membrane C (PDMS) prepared by coating of the ceramic support with [Emim][Ac]: high ideal CO<sub>2</sub>/N<sub>2</sub> selectivity of 152 and permeability of 2400 barrer. These results lie above the literature data and above the Robeson upper bound correlation.

The results for membranes A and B, impregnated by coating with [Emim][Ac] and [Emim][BF<sub>4</sub>], respectively, lie below the Robeson upper bound correlation. For membrane A, the ideal CO<sub>2</sub>/N<sub>2</sub> selectivity and permeability were 24 and 140 barrer and for membrane B, 45 and 90 barrer, respectively.

The main disadvantage of the SILMs is their insufficient stability, which is important in the case of large-scale industrial applications and long-time operations [108,109]. The SILM stability depends strongly on the ILs properties and the preparation methods [110,111].

#### 2.4. Comparison of Process Parameters for the Investigated Methods

The general comparison of measured CO<sub>2</sub> sorption capacities and CO<sub>2</sub> molar fluxes for the investigated methods of CO<sub>2</sub> removal is presented in Table 3. The comparison was made for the following experimental conditions: temperature of 40 °C, atmospheric pressure, ionic liquid [Emim][Ac] as a CO<sub>2</sub> solvent and inlet CO<sub>2</sub> concentration 12–15% vol. Calculated CO<sub>2</sub> sorption capacity *S* represents the mass (kg) of absorbed CO<sub>2</sub> per mass (kg) of IL or the bed for absorption or adsorption, respectively, during the time of the experiment.

As can be seen in the case of [Emim][Ac] as a CO<sub>2</sub> solvent, the absorption in the packed column allows for obtaining high sorption capacities and molar fluxes. For membrane separation, high selectivity  $\alpha$  was measured, but CO<sub>2</sub> molar fluxes were very low. For adsorption, the measured values were rather small but comparable with the literature data. Maximum absorption or adsorption capacity *S* was obtained for saturation of [Emim][Ac] with pure CO<sub>2</sub> for about 8 h.

Regeneration step in the case of absorption of CO<sub>2</sub> in pure IL was made by heating of IL at 95 °C under vacuum for 12 h. For absorption in a packed column, the regeneration was made “in situ” at a temperature of 90 °C with inert gas (nitrogen) flow, for 12 h. For adsorption in the packed column, the regeneration step was performed by heating of the bed in an electric oven at the temperature of 120 °C, for 24 h. In the case of membrane separation, some of the prepared SILMs lost their separation properties because of the

loss of IL from the pores of the ceramic support at elevated pressures. It is possible to use the same ceramic support again for the same IL by additional impregnation with IL, but it needs a special effort to clean and prepare the membrane. Such experiments were performed, but it is easier and safer to prepare the new membrane.

**Table 3.** Comparison of process parameters for the investigated methods of CO<sub>2</sub> removal at 40 °C and atmospheric pressure.

Investigated Methods with [Emim][Ac]	C <sub>in</sub> (CO <sub>2</sub> % vol.)	Gas Flow, V (l <sup>3</sup> /h)	P (atm)	N·10 <sup>6</sup> (kmol m <sup>-2</sup> s <sup>-1</sup> )	S (kg CO <sub>2</sub> /kg Sorbent)/α	Regeneration Step
Absorption in pure liquid	100	36	near atmospheric	-	s = 0.086	thermal t = 95 °C and vacuum
Absorption in packed column	15	138	near atmospheric	0.166	s = 0.053	thermal t = 90 °C with N <sub>2</sub>
Adsorption in packed column	12	750	near atmospheric	0.111	s = 0.013	thermal t = 120 °C
Membrane separation	12	-	2–6	0.025–0.1	α = 10–136	n/a

### 3. Conclusions

The experimental research is presented for different methods of carbon dioxide removal from flue gases: absorption, adsorption and membrane separation under the same or similar experimental conditions, based on commonly used materials: packings, beds, membranes and CO<sub>2</sub> solvents. The experiments were carried out at low pressures and temperatures for the chosen standard imidazolium ILs and the materials were modified by impregnation with IL or amine.

The efficiency comparison of the investigated methods showed that for an SILM based on a ceramic membrane C (PDMS) impregnated with [Emim][Ac] by coating in a vacuum (Figure 10), the best results of long-term stability and permselectivity were obtained with a high value of ideal selectivity and permeability 152 and 2400 barrer, respectively. High separation coefficient values can be crucial in cases where selectivity is a priority, even when permeate molar fluxes are very low.

Applying commercial tubular ceramic membranes made by Inopor and Pervatech, inexpensive SILMs were prepared by impregnating them with selected ionic liquids by coating or soaking methods. For the prepared SILMs, CO<sub>2</sub> molar fluxes increase and the ideal CO<sub>2</sub>/N<sub>2</sub> selectivities decrease with the increasing pressure difference and feed temperature. The low cost of PDMS membranes and the small amount of ionic liquid required for impregnation, coupled with a simple method of IL immobilization in the membrane support make it possible to obtain stable and highly selective SILM membranes.

A presentation of the obtained results in Robeson's plot shows an improvement in separation efficiency and selectivity. The separation performance of SILMs formed by ionic liquid impregnation of membranes A and B made by Inopor is below the limit given by Robeson.

The optimum operating conditions for the tested SILM membranes were a feed temperature of 20 °C and a pressure below 200 kPa. With the higher transmembrane pressures, SILMs lose permselective properties due to degradation.

For CO<sub>2</sub> absorption in a packed column sprayed with IL, gas and liquid flow rates were limited due to the high viscosity of the ionic liquids. For the higher flow rates, an effect of column flooding was observed. The inlet CO<sub>2</sub> concentration and temperature significantly affects the absorption efficiency.

Despite similar carbon dioxide absorption capacities, under the same experimental conditions, the absorption in aqueous MEA solution is much faster than in ionic liquids. This effect is due to the much higher viscosity of ILs rather than amine solutions, so the diffusion coefficient for ILs is lower than for amine solutions.

For CO<sub>2</sub> adsorption on activated carbons, pelletized activated carbon (4 mm) and pelletized activated coconut carbon (4 mm) impregnated with ionic liquid ([Emim][Ac]) or amine (TEDA), respectively, only a small improvement in the adsorption properties was achieved.

The comparison of investigated methods (Table 3), taking into account [Emim][Ac] as a CO<sub>2</sub> solvent, shows that applying a packed column sprayed with IL allows for obtaining high CO<sub>2</sub> sorption capacities and molar fluxes. In the case of membrane separation, high selectivities  $\alpha$  were measured, but CO<sub>2</sub> molar fluxes were low. For adsorption on activated carbons, measured values of CO<sub>2</sub> sorption capacities were rather small, but were comparable with the literature data.

The experimental research and results may represent interesting clues for a decision on which method of carbon dioxide removal will be more efficient for a specific task.

**Author Contributions:** Conceptualization, methodology, validation, investigation, writing—review and editing: Z.Z. and A.R.; writing—original draft preparation: Z.Z.; visualization A.R. All authors have read and agreed to the published version of the manuscript.

**Funding:** This research received no external funding.

**Institutional Review Board Statement:** Not applicable.

**Informed Consent Statement:** Not applicable.

**Conflicts of Interest:** The authors declare no conflict of interest.

## Nomenclature

barrer	non-SI unit of gas permeability; 1 barrer = $3.35 \times 10^{-16}$ (mol m s <sup>-1</sup> Pa <sup>-1</sup> m <sup>-2</sup> )
D	membrane diffusion coefficient, m <sup>2</sup> s <sup>-1</sup>
l	membrane thickness, m
N	molar flux, kmol m <sup>-2</sup> s <sup>-1</sup>
P	permeability, kmol m <sup>-1</sup> s <sup>-1</sup> Pa <sup>-1</sup>
p	pressure difference, Pa
s	solubility, kmol m <sup>-3</sup> Pa <sup>-1</sup>
S	sorption capacity, kg CO <sub>2</sub> kg <sup>-1</sup> sorbent
V <sub>g</sub>	gas flow rate, L/h
$\alpha$	ideal selectivity
$\rho$	density, kg m <sup>-3</sup>
Subscripts	
CO <sub>2</sub>	carbon dioxide
i	CO <sub>2</sub> , N <sub>2</sub>
in	inlet
N <sub>2</sub>	nitrogen
out	outlet

## References

- Cozier, M. Recent developments in carbon capture utilisation and storage. *Greenh. Gases Sci. Technol.* **2019**, *9*, 613–616. [CrossRef]
- Bui, M.; Adjiman, C.S.; Bardow, A.; Anthony, E.J.; Boston, A.; Brown, S.; Fennell, P.S.; Fuss, S.; Galindo, A.; Hackett, L.A.; et al. Carbon capture and storage (CCS): The way forward. *Energy Environ. Sci.* **2018**, *11*, 1062–1176. [CrossRef]
- European Commission. 2020 Climate & Energy Package. 2019. Available online: [https://ec.europa.eu/clima/policies/strategies/2020\\_en](https://ec.europa.eu/clima/policies/strategies/2020_en) (accessed on 1 November 2021).
- European Commission. The EU Emissions Trading System (EU ETS). 2019. Available online: [https://ec.europa.eu/clima/sites/clima/files/factsheet\\_ets\\_en.pdf](https://ec.europa.eu/clima/sites/clima/files/factsheet_ets_en.pdf) (accessed on 1 November 2021).
- Ramstein, C.; Dominioni, G.; Ettehad, S.; Lam, L.; Quant, M.; Zhang, J.; Mark, L.; Nierop, S.; Berg, T.; Leuschner, P.; et al. *State and Trends of Carbon Pricing 2019*; World Bank Group: Washington, DC, USA, 2019.
- Fouret, F. What Are the Effects of the Price Increase for the CO<sub>2</sub> Allowances on the EU ETS Market? Beyond Ratings. 2019. Available online: <https://beyond-ratings.com/publications/what-effects-priceincrease-co2-allowances-eu-ets-market> (accessed on 1 November 2021).
- Yoro, K.O.; Daramola, M.O. Chapter 1—CO<sub>2</sub> emission sources, greenhouse gases, and the global warming effect. In *Advances in Carbon Capture*; Rahimpour, M.R., Farsi, M., Makarem, M.A., Eds.; Woodhead Publishing: Shaxton, UK, 2020; pp. 3–28.

8. Mac Dowell, N.; Fennell, P.S.; Shah, N.; Maitland, G.C. The role of CO<sub>2</sub> capture and utilization in mitigating climate change. *Nat. Clim. Change* **2017**, *7*, 243–249. [[CrossRef](#)]
9. Atlassian, A.A.; Kryuchkov, S.S.; Yanbikov, N.R.; Smorodin, K.A.; Petukhov, A.N.; Trubyanov, M.M.; Vorotyntsev, V.M.; Vorotyntsev, I.V. Comprehensive experimental study of acid gases removal process by membrane-assisted gas absorption using imidazolium ionic liquids solutions absorbent. *Sep. Purif. Technol.* **2020**, *239*, 116578. [[CrossRef](#)]
10. Davison, J. Performance and costs of power plants with capture and storage of CO<sub>2</sub>. *Energy* **2007**, *32*, 1163–1176. [[CrossRef](#)]
11. Gulzar, A.; Gulzar, A.; Ansari, M.B.; He, F.; Gai, S.; Yang, P. Carbon dioxide utilization: A paradigm shift with CO<sub>2</sub> economy. *Chem. Eng. J. Adv.* **2020**, *3*, 100013. [[CrossRef](#)]
12. Kanniche, M.; Gros-Bonnivard, R.; Jaud, P.; Valle-Marcos, J.; Amann, J.M.; Bouallou, C. Pre-combustion, post-combustion and oxy-combustion in thermal power plant for CO<sub>2</sub> capture. *Appl. Therm. Eng.* **2010**, *30*, 53–62. [[CrossRef](#)]
13. Klingberg, P.; Wilkner, K.; Schlüter, M.; Grünauer, J.; Shishatskiy, S. Separation of Carbon Dioxide from Real Power Plant Flue Gases by Gas Permeation Using a Supported Ionic Liquid Membrane: An Investigation of Membrane Stability. *Membranes* **2019**, *9*, 35. [[CrossRef](#)]
14. Sasikumar, B.; Arthanareeswaran, G.; Ismail, A. Recent progress in ionic liquid membranes for gas separation. *J. Mol. Liq.* **2018**, *266*, 330–341. [[CrossRef](#)]
15. Martin-Gil, V.; Ahmad, M.Z.; Castro-Muñoz, R.; Fila, V. Economic Framework of Membrane Technologies for Natural Gas Applications. *Sep. Purif. Rev.* **2018**, *48*, 298–324. [[CrossRef](#)]
16. Fatima, S.S.; Borhan, A.; Ayoub, M.; Ghani, N.A. Development and progress of functionalized silica-based adsorbents for CO<sub>2</sub> capture. *J. Mol. Liq.* **2021**, *338*, 116913. [[CrossRef](#)]
17. Rochelle, G.T. Amine Scrubbing for CO<sub>2</sub> Capture. *Science* **2009**, *325*, 1652–1654. [[CrossRef](#)]
18. Coleman, C. A policy analysis of the driving factors behind carbon capture and storage facilities. *LSU J. Energy L. Resour.* **2018**, *6*, 557.
19. Budzianowski, W. Explorative analysis of advanced solvent processes for energy efficient carbon dioxide capture by gas–liquid absorption. *Int. J. Greenh. Gas Control* **2016**, *49*, 108–120. [[CrossRef](#)]
20. Zhao, B.; Sun, Y.; Yuan, Y.; Gao, J.; Wang, S.; Zhuo, Y.; Chen, C. Study on corrosion in CO<sub>2</sub> chemical absorption process using amine solution. *Energy Procedia* **2011**, *4*, 93–100. [[CrossRef](#)]
21. Huang, Y.; Zhang, X.; Zhang, X.; Dong, H.; Zhang, S. Thermodynamic Modeling and Assessment of Ionic Liquid-Based CO<sub>2</sub> Capture Processes. *Ind. Eng. Chem. Res.* **2014**, *53*, 11805–11817. [[CrossRef](#)]
22. Leung, D.Y.C.; Caramanna, G.; Maroto-Valer, M.M. An overview of current status of carbon dioxide capture and storage technologies. *Renew. Sustain. Energy Rev.* **2014**, *39*, 426–443. [[CrossRef](#)]
23. Wang, M.; Joel, A.S.; Ramshaw, C.; Eimer, D.; Musa, N.M. Process intensification for post-combustion CO<sub>2</sub> capture with chemical absorption: A critical review. *Appl. Energy* **2015**, *158*, 275–291. [[CrossRef](#)]
24. Ramdin, M.; de Loos, T.W.; Vlught, T.J. State-of-the-Art of CO<sub>2</sub> Capture with Ionic Liquids. *Ind. Eng. Chem. Res.* **2012**, *51*, 8149–8177. [[CrossRef](#)]
25. Lucquiaud, M.; Liang, X.; Errey, O.; Chalmers, H.; Gibbins, J. Addressing Technology Uncertainties in Power Plants with Post-Combustion Capture. *Energy Procedia* **2013**, *37*, 2359–2368. [[CrossRef](#)]
26. Jackson, S.; Brodal, E. Optimization of the Energy Consumption of a Carbon Capture and Sequestration Related Carbon Dioxide Compression Processes. *Energies* **2019**, *12*, 1603. [[CrossRef](#)]
27. Luis, P. Use of monoethanolamine (MEA) for CO<sub>2</sub> capture in a global scenario: Consequences and alternatives. *Desalination* **2016**, *380*, 93–99. [[CrossRef](#)]
28. Li, K.; Cousins, A.; Yu, H.; Feron, P.; Tade, M.; Luo, W.; Chen, J. Systematic study of aqueous monoethanolamine-based CO<sub>2</sub> capture process: Model development and process improvement. *Energy Sci. Eng.* **2016**, *4*, 23–39. [[CrossRef](#)]
29. Liu, L.; Wang, S.; Niu, H.; Gao, S. Process and Integration Optimization of Post-Combustion CO<sub>2</sub> Capture System in a Coal Power Plant. *Energy Procedia* **2018**, *154*, 86–93. [[CrossRef](#)]
30. De Guido, G.; Compagnoni, M.; Pellegrini, L.A.; Rossetti, I. Mature versus emerging technologies for CO<sub>2</sub> capture in power plants: Key open issues in post-combustion amine scrubbing and in chemical looping combustion. *Front. Chem. Sci. Eng.* **2018**, *12*, 315–325. [[CrossRef](#)]
31. Budinis, S.; Krevor, S.; Mac Dowell, N.; Brandon, N.; Hawkes, A. An assessment of CCS costs, barriers and potential. *Energy Strat. Rev.* **2018**, *22*, 61–81. [[CrossRef](#)]
32. Nakao, S.I.; Yogo, K.; Goto, K.; Kai, T.; Yamada, H. *Advanced CO<sub>2</sub> Capture Technologies: Absorption, Adsorption, and Membrane Separation Methods*; Springer: New York, NY, USA, 2019.
33. Sarmad, S.; Mikkola, J.P.; Ji, X. CO<sub>2</sub> Capture with Ionic Liquids (ILs) and Deep Eutectic Solvents (DESs): A New Generation of Sorbents. *ChemSusChem* **2017**, *10*, 324–352. [[CrossRef](#)]
34. Haghbakhsh, R.; Raeissi, S.; Parvaneh, K.; Shariati, A. The friction theory for modeling the viscosities of deep eutectic solvents using the CPA and PC-SAFT equations of state. *J. Mol. Liq.* **2018**, *249*, 554–561. [[CrossRef](#)]
35. Haghbakhsh, R.; Parvaneh, K.; Raeissi, S.; Shariati, A. A general viscosity model for deep eutectic solvents: The free volume theory coupled with association equations of state. *Fluid Phase Equilibria* **2018**, *470*, 193–202. [[CrossRef](#)]
36. Blatha, J.; Deublerb, N.; Hirtha, T.; Schiestelb, T. Chemisorption of carbon dioxide in imidazolium based ionic liquids with carboxylic anions. *Chem. Eng. J.* **2012**, *181–182*, 152–158. [[CrossRef](#)]

37. Aghaie, M.; Rezaei, N.; Zendejboudi, S. A systematic review on CO<sub>2</sub> capture with ionic liquids: Current status and future prospects. *Renew. Sustain. Energy Rev.* **2018**, *96*, 502–525. [[CrossRef](#)]
38. Shukla, S.K.; Khokarale, S.G.; Bui, T.Q.; Mikkola, J.-P.T. Ionic Liquids: Potential Materials for Carbon Dioxide Capture and Utilization. *Front. Mater.* **2019**, *6*, 1–8. [[CrossRef](#)]
39. Ma, C.; Sarmad, S.; Mikkola, J.-P.; Ji, X. Development of Low-Cost Deep Eutectic Solvents for CO<sub>2</sub> Capture. *Energy Procedia* **2017**, *142*, 3320–3325. [[CrossRef](#)]
40. Florindo, C.; Lima, F.; Ribeiro, B.D.; Marrucho, I.M. Deep eutectic solvents: Overcoming 21st century challenges. *Curr. Opin. Green Sustain. Chem.* **2019**, *18*, 31–36. [[CrossRef](#)]
41. Alkhatib, I.I.I.; Ferreira, M.L.; Alba, C.G.; Bahamon, D.; Llovel, F.; Pereiro, A.B.; Araújo, J.M.M.; Abu-Zahra, M.R.; Vega, L.F. Screening of Ionic Liquids and Deep Eutectic Solvents for Physical CO<sub>2</sub> Absorption by Soft-SAFT Using Key Performance Indicators. *J. Chem. Eng. Data* **2020**, *65*, 5844–5861. [[CrossRef](#)]
42. Strazisar, B.R.; Anderson, A.R.R.; White, C.M. Degradation Pathways for Monoethanolamine in a CO<sub>2</sub> Capture Facility. *Energy Fuels* **2003**, *17*, 1034–1039. [[CrossRef](#)]
43. Dubois, L.; Thomas, D. Screening of Aqueous Amine-Based Solvents for Postcombustion CO<sub>2</sub> Capture by Chemical Absorption. *Chem. Eng. Technol.* **2012**, *35*, 513–524. [[CrossRef](#)]
44. Bara, J.E. Ionic liquids for post combustion CO<sub>2</sub> capture. In *Absorption Based Post-Combustion Capture of Carbon Dioxide*; Feron, P.H.M., Ed.; Woodhead Publishing: Duxford, UK, 2016.
45. Yokozeki, A.; Shiflett, M.B.; Junk, C.P.; Grieco, L.M.; Foo, T. Physical and Chemical Absorptions of Carbon Dioxide in Room-Temperature Ionic Liquids. *J. Phys. Chem. B* **2008**, *112*, 16654–16663. [[CrossRef](#)] [[PubMed](#)]
46. Gurau, G.; Rodríguez, H.; Kelley, S.P.; Janiczek, P.; Kalb, R.S.; Rogers, R.D. Demonstration of Chemisorption of Carbon Dioxide in 1,3-Dialkylimidazolium Acetate Ionic Liquids. *Angew. Chem. Int. Ed.* **2011**, *50*, 12024–12026. [[CrossRef](#)] [[PubMed](#)]
47. Janiczek, P.; Kalb, R.S.; Thonhauser, G.; Gamse, T. Carbon dioxide absorption in a technical-scale-plant utilizing an imidazolium-based ionic liquid. *Sep. Purif. Technol.* **2012**, *97*, 20–25. [[CrossRef](#)]
48. Shiflett, M.B.; Yokozeki, A. Phase behavior of carbon dioxide in ionic liquids: [Emim][Acetate], [Emim][Trifluoroacetate], and [Emim][Acetate][Emim][Tri-fluoroacetate] mixtures. *J. Chem. Eng. Data* **2009**, *54*, 108–114. [[CrossRef](#)]
49. Shiflett, M.B.; Niehaus, A.M.S.; Elliott, B.A.; Yokozeki, A. Phase Behavior of N<sub>2</sub>O and CO<sub>2</sub> in Room-Temperature Ionic Liquids [bmim][Tf<sub>2</sub>N], [bmim][BF<sub>4</sub>], [bmim][N(CN)<sub>2</sub>], [bmim][Ac], [eam][NO<sub>3</sub>], and [bmim][SCN]. *Int. J. Thermophys.* **2012**, *33*, 412–436. [[CrossRef](#)]
50. Zhang, J.; Zhang, S.; Dong, K.; Zhang, Y.; Shen, Y.; Lv, X. Supported Absorption of CO<sub>2</sub> by Tetrabutylphosphonium Amino Acid Ionic Liquids. *Chem.-A Eur. J.* **2006**, *12*, 4021–4026. [[CrossRef](#)] [[PubMed](#)]
51. Fukumoto, K.; Yoshizawa, M.; Ohno, H. Room Temperature Ionic Liquids from 20 Natural Amino Acids. *J. Am. Chem. Soc.* **2005**, *127*, 2398–2399. [[CrossRef](#)] [[PubMed](#)]
52. Zhang, Y.; Zhang, S.; Lu, X.; Zhou, Q.; Fan, W.; Zhang, X. Dual Amino-Functionalised Phosphonium Ionic Liquids for CO<sub>2</sub> Capture. *Chem.-A Eur. J.* **2009**, *15*, 3003–3011. [[CrossRef](#)] [[PubMed](#)]
53. Shiflett, M.B.; Drew, D.W.; Cantini, R.A.; Yokozeki, A. Carbon Dioxide Capture Using Ionic Liquid 1-Butyl-3-methylimidazolium Acetate. *Energy Fuels* **2010**, *24*, 5781–5789. [[CrossRef](#)]
54. Khonkaen, K.; Siemanond, K.; Henni, A. Simulation of Carbon Dioxide Capture Using Ionic Liquid 1-Ethyl-3-methylimidazolium Acetate. In *Computer Aided Chemical Engineering, Proceedings of the 24th European Symposium on Computer Aided Process Engineering, Budapest, Hungary, 15–18 June 2014*; Elsevier: Amsterdam, The Netherlands, 2014; Volume 33, pp. 1045–1050.
55. Bhowan, A.S.; Freeman, B.C. Analysis and Status of Post-Combustion Carbon Dioxide Capture Technologies. *Environ. Sci. Technol.* **2011**, *45*, 8624–8632. [[CrossRef](#)] [[PubMed](#)]
56. Wu, Y.; Xu, J.; Mumford, K.; Stevens, G.W.; Fei, W.; Wang, Y. Recent advances in carbon dioxide capture and utilization with amines and ionic liquids. *Green Chem. Eng.* **2020**, *1*, 16–32. [[CrossRef](#)]
57. Yoro, K.O.; Daramola, M.O.; Sekoai, P.T.; Armah, E.K.; Wilson, U.N. Advances and emerging techniques for energy recovery during absorptive CO<sub>2</sub> capture: A review of process and non-process integration-based strategies. *Renew. Sustain. Energy Rev.* **2021**, *147*, 111241. [[CrossRef](#)]
58. Yang, H.; Xu, Z.; Fan, M.; Gupta, R.; Slimane, R.B.; Bland, A.E.; Wright, I. Progress in carbon dioxide separation and capture: A review. *J. Environ. Sci.* **2008**, *20*, 14–27. [[CrossRef](#)]
59. Pevida, C.; Plaza, M.G.; Arias, B.; Feroso, J.; Rubiera, F.; Pis, J.J. Surface modification of activated carbons for CO<sub>2</sub> capture. *Appl. Surf. Sci.* **2008**, *254*, 7165–7172. [[CrossRef](#)]
60. El Gamal, M.; Mousa, H.A.; El-Naas, M.H.; Zacharia, R.; Judd, S. Bio-regeneration of activated carbon: A comprehensive review. *Sep. Purif. Technol.* **2018**, *197*, 345–359. [[CrossRef](#)]
61. Rehman, A.; Park, M.; Park, S.-J. Current Progress on the Surface Chemical Modification of Carbonaceous Materials. *Coatings* **2019**, *9*, 103. [[CrossRef](#)]
62. He, X.; Zhu, J.; Wang, H.; Zhou, M.; Zhang, S. Surface Functionalization of Activated Carbon with Phosphonium Ionic Liquid for CO<sub>2</sub> Adsorption. *Coatings* **2019**, *9*, 590. [[CrossRef](#)]
63. Ramli, A.; Ahmed, S.; Yusup, S. Adsorption behavior of Si-MCM-41 for CO<sub>2</sub>: Effect of pressure and temperature on adsorption. *Chem. Eng. Trans.* **2014**, *39*, 271–276.

64. Satyapal, S.; Filburn, T.; Trela, J.; Strange, J. Performance and Properties of a Solid Amine Sorbent for Carbon Dioxide Removal in Space Life Support Applications. *Energy Fuels* **2001**, *15*, 250–255. [[CrossRef](#)]
65. Hiremath, V.; Jadhav, A.H.; Lee, H.; Kwon, S.; Gil Seo, J. Highly reversible CO<sub>2</sub> capture using amino acid functionalized ionic liquids immobilized on mesoporous silica. *Chem. Eng. J.* **2016**, *287*, 602–617. [[CrossRef](#)]
66. Zhang, W.; Gao, E.; Li, Y.; Bernards, M.; He, Y.; Shi, Y. CO<sub>2</sub> capture with polyamine-based protic ionic liquid functionalized mesoporous silica. *J. CO<sub>2</sub> Util.* **2019**, *34*, 606–615. [[CrossRef](#)]
67. Girish, C.R. Various Impregnation Methods Used for the Surface Modification of the Adsorbent: A Review. *Int. J. Eng. Technol.* **2018**, *7*, 330–334. [[CrossRef](#)]
68. Cecilia, J.; Vilarrasa-García, E.; García-Sancho, C.; Saboya, R.; Azevedo, D.; Cavalcante, C.; Rodríguez-Castellón, E. Functionalization of hollow silica microspheres by impregnation or grafted of amine groups for the CO<sub>2</sub> capture. *Int. J. Greenh. Gas Control.* **2016**, *52*, 344–356. [[CrossRef](#)]
69. Shankar, K.; Kandasamy, P. Carbon dioxide separation using  $\alpha$ -alumina ceramic tube supported cellulose triacetate-tributyl phosphate composite membrane. *Greenh. Gases Sci. Technol.* **2019**, *9*, 287–305. [[CrossRef](#)]
70. Kárászová, M.; Zach, B.; Petrusová, Z.; Červenka, V.; Bobák, M.; Šyc, M.; Izák, P. Post-combustion carbon capture by membrane separation. *Review. Sep. Purif. Technol.* **2020**, *238*, 116448. [[CrossRef](#)]
71. Yan, X.; Anguille, S.; Bendahan, M.; Moulin, P. Ionic liquids combined with membrane separation processes: A review. *Sep. Purif. Technol.* **2019**, *222*, 230–253. [[CrossRef](#)]
72. Vakharia, V.; Salim, W.; Wu, D.; Han, Y.; Chen, Y.; Zhao, L.; Ho, W.W. Scale-up of amine-containing thin-film composite membranes for CO<sub>2</sub> capture from flue gas. *J. Membr. Sci.* **2018**, *555*, 379–387. [[CrossRef](#)]
73. AlQaheem, Y.; Alomair, A.; Vinoba, M.; Pérez, A. Polymeric Gas-Separation Membranes for Petroleum Refining. *Int. J. Polym. Sci.* **2017**, *2017*, 1–19. [[CrossRef](#)]
74. Xu, J.; Wang, Z.; Qiao, Z.; Wu, H.; Dong, S.; Zhao, S.; Wang, J. Post-combustion CO<sub>2</sub> capture with membrane process: Practical membrane performance and appropriate pressure. *J. Membr. Sci.* **2019**, *581*, 195–213. [[CrossRef](#)]
75. Roussanaly, S.; Anantharaman, R.; Lindqvist, K.; Hagen, B. A new approach to the identification of high-potential materials for cost-efficient membrane-based post-combustion CO<sub>2</sub> capture. *Sustain. Energy Fuels* **2018**, *2*, 1225–1243. [[CrossRef](#)]
76. Xu, J.; Jia, H.; Yang, N.; Wang, Q.; Yang, G.; Zhang, M.; Xu, S.; Zang, Y.; Ma, L.; Jiang, P.; et al. High Efficiency Gas Permeability Membranes from Ethyl Cellulose Grafted with Ionic Liquids. *Polymers* **2019**, *11*, 1900. [[CrossRef](#)]
77. Chatterjee, G.; Houde, A.A.; Stern, S.A. Poly(etherurethane) and poly(ether urethane urea) membranes with high H<sub>2</sub>S/CH<sub>4</sub> selectivity. *J. Membr. Sci.* **1997**, *135*, 99–106. [[CrossRef](#)]
78. Bernardo, P.; Drioli, E.; Golemme, G. Membrane Gas Separation: A Review/State of the Art. *Ind. Eng. Chem. Res.* **2009**, *48*, 4638–4663. [[CrossRef](#)]
79. Ismail, A.; Khulbe, K.; Matsuura, T. *Gas Separation Membranes: Polymeric and Inorganic*; Springer: Heidelberg, Germany, 2015.
80. Amooghini, A.E.; Omidkhan, M.; Kargari, A. Enhanced CO<sub>2</sub> transport properties of membranes by embedding nano-porous zeolite particles into Matrimid®5218 matrix. *RSC Adv.* **2015**, *5*, 8552–8565. [[CrossRef](#)]
81. Liu, S.; Wang, R.; Liu, Y.; Chng, M.; Chung, N.T.-S. The physical and gas permeation properties of 6FDA-durene/2,6-diaminotoluene copolyimides. *Polymers* **2001**, *42*, 8847–8855. [[CrossRef](#)]
82. Scholes, C.A.; Chen, G.Q.; Lu, H.T.; Kentish, S.E. Crosslinked PEG and PEBAX Membranes for Concurrent Permeation of Water and Carbon Dioxide. *Membranes* **2016**, *6*, 1. [[CrossRef](#)] [[PubMed](#)]
83. Amooghini, A.E.; Sanaeepur, H.; Pedram, M.Z.; Omidkhan, M.; Kargari, A. New advances in polymeric membranes for CO<sub>2</sub> separation. In *Polymer Science: Research Advances, Practical Applications and Educational Aspects*; Vilas, A.M., Martin, A.S., Eds.; Formatec Research Center S.L.: Badajoz, Spain, 2016; pp. 354–368. ISBN 978-8494213489.
84. Salih, A.A.; Yi, C.; Peng, H.; Yang, B.; Yin, L.; Wang, W. Interfacially polymerized polyetheramine thin film composite membranes with PDMS inter-layer for CO<sub>2</sub> separation. *J. Membr. Sci.* **2014**, *472*, 110–118. [[CrossRef](#)]
85. Pian, C.; Shen, J.; Liu, G.; Liu, Z.; Jin, W. Ceramic hollow fiber-supported PDMS composite membranes for oxygen enrichment from air. *Asia-Pac. J. Chem. Eng.* **2016**, *11*, 460–466. [[CrossRef](#)]
86. Mark, J.E.; Allcock, H.R.; West, R. *Inorganic Polymers*, 2nd ed.; Oxford University Press: New York, NY, USA, 2005.
87. Sadrzadeh, M.; Shahidi, K.; Mohammadi, T. Synthesis and gas permeation properties of a single layer PDMS membrane. *J. Appl. Polym. Sci.* **2010**, *117*, 33–48. [[CrossRef](#)]
88. Ahmad, M.Z.; Fuoco, A. Porous liquids—Future for CO<sub>2</sub> capture and separation? *Curr. Res. Green Sustain. Chem.* **2021**, *4*, 100070. [[CrossRef](#)]
89. Camper, D.; Bara, J.E.; Gin, D.L.; Noble, R.D. Room-Temperature Ionic Liquid—Amine Solutions: Tunable Solvents for Efficient and Reversible Capture of CO<sub>2</sub>. *Ind. Eng. Chem. Res.* **2008**, *47*, 8496–8498. [[CrossRef](#)]
90. Xie, Y.; Zhang, Y.; Lu, X.; Ji, X. Energy consumption analysis for CO<sub>2</sub> separation using imidazolium-based ionic liquids. *Appl. Energy* **2014**, *136*, 325–335. [[CrossRef](#)]
91. Chakma, A. CO<sub>2</sub> capture processes—Opportunities for improved energy efficiencies. *Energy Convers. Manag.* **1997**, *38*, S51–S56. [[CrossRef](#)]
92. Cserjési, P.; Nemestóthy, N.; Bélafi-Bakó, K. Gas separation properties of supported liquid membranes prepared with unconventional ionic liquids. *J. Membr. Sci.* **2010**, *349*, 6–11. [[CrossRef](#)]
93. Santos, E.; Albo, J.; Irabien, A. Acetate based Supported Ionic Liquid Membranes (SILMs) for CO<sub>2</sub> separation: Influence of the temperature. *J. Membr. Sci.* **2014**, *452*, 277–283. [[CrossRef](#)]

94. Bara, J.; Carlisle, T.K.; Gabriel, C.J.; Camper, D.; Finotello, A.; Gin, D.; Noble, R.D. Guide to CO<sub>2</sub> Separations in Imidazolium-Based Room-Temperature Ionic Liquids. *Ind. Eng. Chem. Res.* **2009**, *48*, 2739–2751. [[CrossRef](#)]
95. Albo, J.; Yoshioka, T.; Tsuru, T. Porous Al<sub>2</sub>O<sub>3</sub>/TiO<sub>2</sub> tubes in combination with 1-ethyl-3-methylimidazolium acetate ionic liquid for CO<sub>2</sub>/N<sub>2</sub> separation. *Sep. Purif. Technol.* **2014**, *122*, 440–448. [[CrossRef](#)]
96. Sánchez Fuentes, C.E.; Guzmán-Lucero, D.; Torres-Rodriguez, M.; Likhanova, N.V.; Navarrete Bolaños, J.; Olivares-Xometl, O.; Lijanová, I.V. CO<sub>2</sub>/N<sub>2</sub> separation using alumina supported membranes based on new functionalized ionic liquids. *Sep. Purif. Technol.* **2017**, *182*, 59–68. [[CrossRef](#)]
97. Khraisheh, M.; Zadeh, K.M.; Alkhouzaam, A.; Turki, D.; Hassan, M.K.; Al Momani, F.; Zaidi, S.M.J. Characterization of polysulfone/diisopropylamine 1-alkyl-3-methylimidazolium ionic liquid membranes: High pressure gas separation applications. *Greenh. Gases Sci. Technol.* **2020**, *10*, 795–808. [[CrossRef](#)]
98. Karousos, D.S.; Labropoulos, A.I.; Tziaila, O.; Papadokostaki, K.; Gjoka, M.; Stefanopoulos, K.L.; Beltsios, K.G.; Iliev, B.; Schubert, T.J.S.; Romanos, G.E. Effect of a cyclic heating process on the CO<sub>2</sub>/N<sub>2</sub> separation performance and structure of a ceramic nanoporous membrane supporting the ionic liquid 1-methyl-3-octylimidazolium tricyanomethanide. *Sep. Purif. Technol.* **2018**, *200*, 11–22. [[CrossRef](#)]
99. Ziobrowski, Z.; Rotkegel, A. The influence of water content in imidazolium based ILs on carbon dioxide removal efficiency. *Sep. Purif. Technol.* **2017**, *179*, 412–419. [[CrossRef](#)]
100. Ziobrowski, Z.; Krupiczka, R.; Rotkegel, A. Carbon dioxide absorption in a packed column using imidazolium based ionic liquids and MEA solution. *Int. J. Greenh. Gas Control.* **2016**, *47*, 8–16. [[CrossRef](#)]
101. Ziobrowski, Z.; Rotkegel, A. Feasibility study of CO<sub>2</sub>/N<sub>2</sub> separation intensification on supported ionic liquid membranes by commonly used impregnation methods. *Greenh. Gases Sci. Technol.* **2021**, *11*, 297–312. [[CrossRef](#)]
102. Luis, P.; Neves, L.; Afonso, C.A.M.; Coelho, I.; Crespo, J.; Garea, A.; Irbien, A. Facilitated transport of CO<sub>2</sub> and SO<sub>2</sub> through Supported Ionic Liquid Membranes (SILMs). *Desalination* **2009**, *245*, 485–493. [[CrossRef](#)]
103. Freire, M.G.; Teles, A.R.R.; Rocha, M.A.A.; Schröder, B.; Neves, C.M.S.S.; Carvalho, P.J.; Evtuguin, D.V.; Santos, L.M.N.B.F.; Coutinho, J.A.P. Thermophysical Characterization of Ionic Liquids Able To Dissolve Biomass. *J. Chem. Eng. Data* **2011**, *56*, 4813–4822. [[CrossRef](#)]
104. Kreiter, R.; Overbeek, J.P.; Correia, L.A.; Vente, J.F. Pressure resistance of thin ionic liquid membranes using tailored ceramic supports. *J. Membr. Sci.* **2011**, *370*, 175–178. [[CrossRef](#)]
105. Close, J.J.; Farmer, K.; Moganty, S.S.; Baltus, R.E. CO<sub>2</sub>/N<sub>2</sub> separations using nanoporous alumina-supported ionic liquid membranes: Effect of the support on separation performance. *J. Membr. Sci.* **2012**, *390–391*, 201–210. [[CrossRef](#)]
106. Barghi, S.; Adibi, M.; Rashtchian, D. An experimental study on permeability, diffusivity, and selectivity of CO<sub>2</sub> and CH<sub>4</sub> through [bmim][PF<sub>6</sub>] ionic liquid supported on an alumina membrane: Investigation of temperature fluctuations effects. *J. Membr. Sci.* **2010**, *362*, 346–352. [[CrossRef](#)]
107. Robeson, L.M. The upper bound revisited. *J. Membr. Sci.* **2008**, *320*, 390–400. [[CrossRef](#)]
108. Wang, J.; Luo, J.; Feng, S.; Li, H.; Wan, Y.; Zhang, X. Recent development of ionic liquid membranes. *Green Energy Environ.* **2016**, *1*, 43–61. [[CrossRef](#)]
109. Tomé, L.C.; Marrucho, I.M. Ionic liquid-based materials: A platform to design engineered CO<sub>2</sub> separation membranes. *Chem. Soc. Rev.* **2016**, *45*, 2785–2824. [[CrossRef](#)] [[PubMed](#)]
110. Fortunato, R.; Afonso, C.A.M.; Reis, M.A.; Crespo, J.G. Supported liquid membranes using ionic liquids: Study of stability and transport mechanisms. *J. Membr. Sci.* **2004**, *242*, 197–209. [[CrossRef](#)]
111. Hernández-Fernández, F.J.; de los Rios, A.P.; Tomás-Alonso, F.; Palacios, J.M.; Villora, G. Preparation of supported ionic liquid membranes: Influence of the ionic liquid immobilization method on their operational stability. *J. Membr. Sci.* **2009**, *341*, 172–177. [[CrossRef](#)]